

1 Article

# 2 Cellulosic Waste Deriving Filler Content Effect on 3 Biodegradation Behavior and Thermal Properties for 4 HDPE and PLA Composites

5 Alessia Quitadamo<sup>1,2</sup>, Valérie Massardier<sup>2</sup>, Valeria Iovine<sup>1</sup>, Ahmed Belhadji<sup>2</sup>, Rémy Bayard<sup>3</sup>,  
6 Marco Valente<sup>1</sup>

7 <sup>1</sup> Dept. of Chemical and Material Environmental Engineering, Sapienza University of Rome, Italy;  
8 alessia.quitadamo@uniroma1.it, marco.valente@uniroma1.it

9 <sup>2</sup> Université de Lyon, F-69003, INSA de Lyon, F-69621, Villeurbanne, France, CNRS, UMR 5223, Ingénierie  
10 des Matériaux polymers; valerie.massardier@insa-lyon.fr, ahmed.belhadji@insa-lyon.fr

11 <sup>3</sup> Université de Lyon, INSA Lyon, DEEP Laboratory, EA7429, F-69621 Villeurbanne cedex, France;  
12 remy.bayard@insa-lyon.fr

13 \* Correspondence: marco.valente@uniroma1.it

14 **Abstract:** Composites with HDPE and PLA matrix have been tested to analyse the effect of natural  
15 fillers (wood flour, recycled waste paper and a mix of both fillers) and temperature on polymer  
16 degradation. Composting tests have been performed in both mesophilic (35°C) and thermophilic  
17 (58°C) conditions. Degradation development has been evaluated through mass variation, TGA and  
18 DSC. HDPE, as expected, did not display any relevant variation, confirming its stability under our  
19 composting conditions. PLA is sensibly influenced by temperature and humidity, with higher  
20 reduction of Mw when composting is performed at 58°C. Natural fillers seem to influence  
21 degradation process of composites, already at 35°C. In fact, degradation of fillers at 35°C allows a  
22 mass reduction during composting of composites, while neat PLA do not display any variation.

23 **Keywords:** biodegradation; bio-derived polymer; composites

## 25 1. Introduction

26 Degradation is a typical phenomenon of polymer materials leading to fragmentation and  
27 significant changes in the structure of the material characterized by the loss of some properties (e.g.  
28 mechanical properties, viscosity, molecular weight...)[1-2]. Degradation can occur in different ways  
29 such as thermal degradation, photo degradation, oxidative degradation, mechanical degradation,  
30 hydrolysis reaction with water (hydrolytic degradation) and action of microorganisms such as  
31 bacteria, fungi or algae (biodegradation) [3-5].

32 In general, the degradation pathways associated with polymer degradation are often  
33 determined by environmental conditions, depending on aerobiosis (presence of oxygen) or  
34 anaerobiosis (absence of oxygen), and it is based on oxidation or hydrolysis reactions [6-8]. These  
35 reactions can take place simultaneously or in succession. Anaerobic biodegradation is characterized  
36 by three main phases: firstly, hydrolysis occurs, making available molecules for bacteria digestion,  
37 secondly acid and acetogenesis convert sugars and amino acids into CO<sub>2</sub>, H<sub>2</sub>, NH<sub>3</sub> and acetic acid  
38 [9-10]. Finally, methanogenesis produces methane, CO<sub>2</sub> and water. Macroscopically, biodegradation  
39 appears as yellowing, fragmentation and breakage [11]. Aerobic degradation, when O<sub>2</sub> is available,  
40 is characterized by the decomposition of polymers by oxidation which can be followed by hydrolysis  
41 of the oxidation products whose final products will be microbial biomass, CO<sub>2</sub> and H<sub>2</sub>O.  
42 Biodegradability can be evaluated through several standards, depending on the final application of  
43 the tested materials. Several studies have been performed in order to evaluate biodegradability  
44 behavior of bio-derived polymers and composites, or to verify the effect of pro-oxidant on oil-based  
45 polymers [12-14]. The purpose of this work is to evaluate the effect of natural fillers on  
46 biodegradability of bio-derived and oil-based polymers. In 1993, Sinclair et al. already [15] patented

47 blends of polylactic acids with traditional oil-based polymers, aiming to produce blends with  
48 environmentally degradable features. They obtained partially degradable materials, in which PLA  
49 rapidly decomposed, compared to stable traditional polymers. The interesting aspect is the higher  
50 rapidity of degradation of these blends in comparison to conventional non-degradable plastics  
51 because of two simultaneous aspects: firstly, PLA degradation, secondly this degradation allows the  
52 formation of high specific surface area that is expected to accelerate the process. Environmental  
53 consciousness has attracted many interests during last years, directing researches through the use of  
54 bio-derived polymers and natural fillers [16-18]. In fact, composites with natural fillers gain great  
55 attention during last decades [19-21]. Lignocellulosic fibers are characterized by a chemical  
56 composition influenced by genetic and environmental factors. In general, lignocellulosic fibers are  
57 mainly composed of cellulose (linear macromolecules of glucose units, the higher the amount of  
58 cellulose the higher the hydrophilicity of the fibers), hemicellulose (composed of several  
59 polysaccharides) and lignin (irregular and insoluble polymer, composed of aromatic units  
60 characterized by highly networked structures) [21-22]. Chemical structure of lignocellulosic fibers  
61 directly affects not just mechanical properties, but also biodegradability. In fact, each constituent of  
62 lignocellulosic fibers can be more or less susceptible to enzymatic hydrolysis, depending on the  
63 particular chemical structure [23]. Generally speaking, biological degradation occurs firstly for  
64 hemicellulose, then amorphous cellulose and lately for crystalline cellulose [24]. In fact, packed  
65 structures are less accessible for microorganisms, preventing macromolecules degradation.  
66 Biodegradation occurs through breakage of  $\beta$  1,4-xylan bonds of hemicellulose by xylanase,  $\beta$  1,4  
67 glycosidic bonds of cellulose by cellulase and lignin biodegradation thanks to ligninolytic fungi  
68 actions.

69 In our work, samples have been subjected to composting in soil for three months at 35°C and  
70 58°C, in order to evaluate their degradation. In particular, HDPE-based and PLA-based composites  
71 have been tested to analyze the effect of natural fillers (wood flour, recycled waste paper and a mix  
72 of both fillers) on polymer degradation. Both mesophilic and thermophilic conditions have been  
73 tested to analyze also temperature influence on composting processes.

## 74 2. Materials and Methods

### 75 2.1. Materials

76 Eraclene MP90, commercial name of high-density polyethylene (HDPE) from ENI (Versalis), has  
77 been selected as oil-based polymer. Among its properties are: a melt flow index (MFI) of 7 g/10 min  
78 (190°C/2.16kg), a nominal mass of 0.96 g/cm<sup>3</sup>, a tensile strength of 21 MPa, a tensile modulus of 1.2  
79 GPa, a Shore D hardness of 50. Poly(lactic acid) (PLA) Ingeo Biopolymer 3251D from Nature Works  
80 was selected as bio-derived thermoplastic polymer, with a MFI of 35 g/10min (190°C/2.16 kg). This  
81 polymer is characterized by density 1.24, crystalline melting temperature in the range 155-170 °C and  
82 a glass transition temperature in the range 55-60°C. La.So.Le/est/Srl (Udine, Italy) provided the WF  
83 (European beech) with dimensions derived from datasheet: >500  $\mu$ m 0-5%, >300  $\mu$ m 20-70%, >180  $\mu$ m  
84 20-80%, <180  $\mu$ m 0-5%. Recycled waste paper, whose production process is deeply described in  
85 another work [20], have been observed with optical microscopy. Average length of 750 $\pm$ 300  $\mu$ m and  
86 diameter of 25 $\pm$ 10  $\mu$ m have been measured. PLA, WF and recycled waste paper were dried one night  
87 at 80°C under vacuum, before processing.

88 A Micro 15 Twin-screw DSM research extruder was used at 180°C, with screw speed of 75 rpm,  
89 N<sub>2</sub> atmosphere and 4 min residence time. The injection molding temperature was 55°C, and pressure  
90 parameters were depending on the formulation specificities because of different viscosities. Disk of  
91 40mm diameters and 1.5mm thickness have been produced.

### 92 2.2. Composting tests

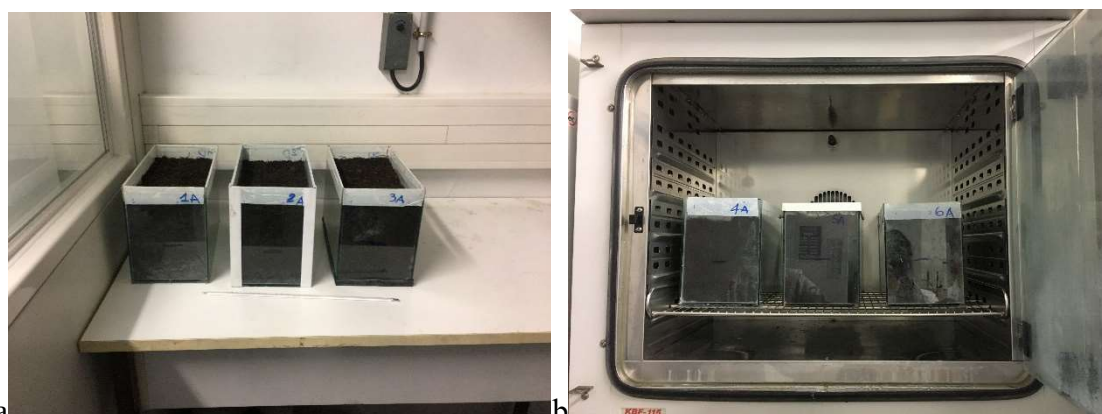
93 Tests were performed in order to analyze the effect of testing temperature, wood flour (WF) and  
94 cellulosic fibers (P) on HDPE and PLA, as well as the behavior of soy protein isolate (with 30% of  
95 glycerol as plasticizer), used as positive reference. Tests duration was three months, keeping samples

96 under both mesophilic (35°C) and thermophilic (58°C) conditions [25]. In each aquarium, 2kg of  
 97 compost have been used: 1 kg has been put at the bottom, samples have been placed and then 1 kg  
 98 of compost has been used to bury samples. During the test humidity has been checked and kept at  
 99 constant value. Before burying, all samples have been dried all night under vacuum at 50°C and  
 100 weighted. Table 1 displays all formulations subjected to this test. Figure 1 displays composting tests  
 101 setup.

102 **Table 1.** Formulations of samples for composting test in soil.

Samples	HDPE (%)	PLA (%)	Wood Flour (WF) (%)	Recycled Waste Paper (P) (%)
HDPE	100			
PLA		100		
HDPE60-WF40	60		40	
HDPE60-P40	60			40
PLA60-WF40		60	40	
PLA60-P40		60		40
PLA60-WF30-P10		60	30	10

103



104

105 **Figure 1.** Composting tests setup at 35°C (a) and 58°C (b).

106 Each month a disk per formulation is taken from the aquarium, washed with distilled water and  
 107 dried until constant weight is reached. The evolution of degradation is analysed by mass variation of  
 108 each samples as:

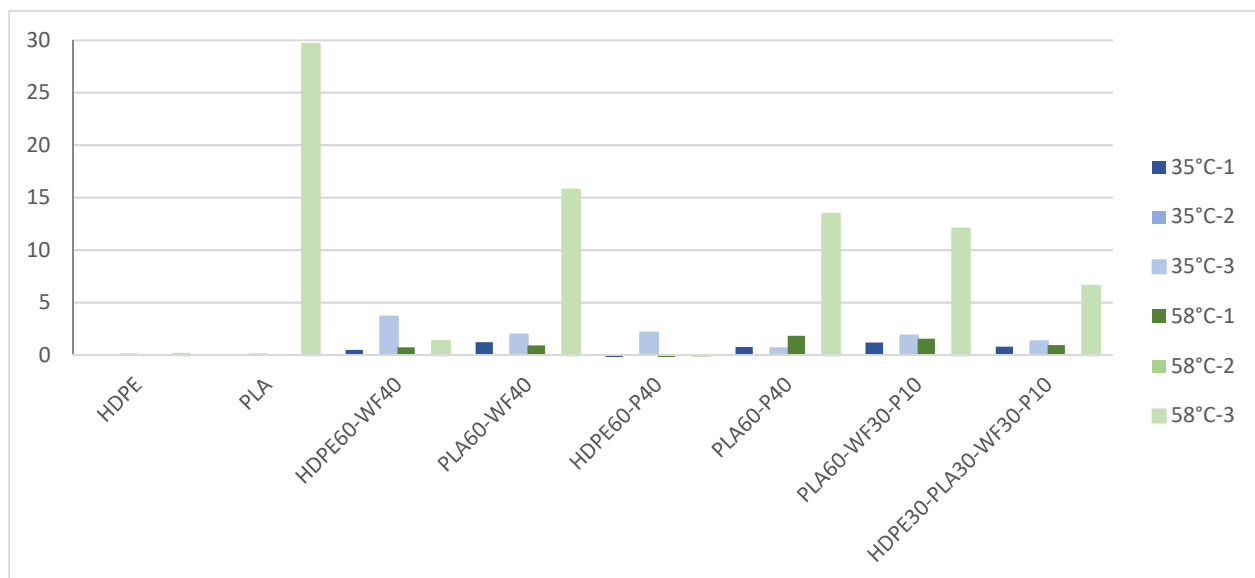
109 
$$\Delta M(\%) = (M_{t0} - M_t) / M_{t0} * 100$$

110 In which  $\Delta M(\%)$  is mass variation,  $M_{t0}$  is mass value before composting and  $M_t$  is mass value at time  
 111  $t$  (respectively 1,2 3 months at 35°C and 58°C). Moreover, other tests have been performed to analyze  
 112 degradation evolution, such as: Thermogravimetric analysis (TGA) carried out on a Q500 Thermal  
 113 Analysis instrument, up to 600°C with a scanning temperature of 10°C·min<sup>-1</sup> under a nitrogen flow  
 114 of 50mL·min<sup>-1</sup> and Differential scanning calorimetry (DSC) performed on a Q20 Thermal Analysis  
 115 instrument with two cycles (with a 4 minutes interval between them) at 180°C to eliminate trace of  
 116 thermal history. The first cycle is carried out from 25°C to 180°C at 10°C·min<sup>-1</sup> under a nitrogen flow  
 117 of 50 mL·min<sup>-1</sup> followed by a cooling from 180°C to 25°C at 10°C·min<sup>-1</sup>  $T_c$  and  $\Delta H_c$  were measured  
 118 during this cooling phase. Then, a second heating from 25°C to 180°C at 10°C·min<sup>-1</sup> enables to

119 determine.  $T_{cc}$ ,  $T_f$  and  $\Delta H_f$ . Infrared Analysis Attenuated Total Reflection (ATR-FTIR) tests were  
 120 carried out with a thermo-scientific Nicolet IS10 spectrometer, with a spectral range 4000-400  $\text{cm}^{-1}$   
 121 and 32 scans.

### 122 3. Results

123 As expected, HDPE displays no mass variation at both 35°C and 58°C, in agreement with  
 124 literature [26], as visible from Figure 2. The addition of wood flour and recycled waste paper  
 125 influenced mass variation. Probably mass variation is related to natural fillers degradation, especially  
 126 for wood flour addition [27]. PLA-based samples, thanks to PLA biodegradability, display mass  
 127 variation, especially after three months at 58°C.



128

129 **Figure 2.** Mass variation measurements of HDPE, PLA, HDPE60-WF40, PLA60-WF40, HDPE60-P40,  
 130 PLA60-P40 and PLA60-WF30-P10 for three months testing in soil at 35°C and 58°C.

131 In agreement with literature results [28], PLA is normally characterized by a first lag phase, in  
 132 which diffusion of water occurs and macromolecules are still too long to be degraded by  
 133 microorganisms. As a consequence, mass variation displays a higher difference for time 3 with  
 134 respect to time 1 and 2. A visible effect of temperature is displayed for neat PLA degradation process.  
 135 In fact, samples at 58°C are characterized by a higher degradation rate and higher mass variation  
 136 with respect to samples at 35°C. PLA degradation is due to breakage of ester bonds. Water  
 137 hydrolyses polymer chains randomly. As a consequence, polymer molecular weight is reduced, and  
 138 oligomers are obtained. In fact, degradation can be evaluated through mass variation [29]. Wood  
 139 flour and recycled waste paper addition seems to increase mass variation for PLA-based samples at  
 140 35°C. This can be related to humidity absorbed by wood flour and recycled waste paper [30].  
 141 Moreover, a degradation of natural fillers can also occur, reducing sample's mass. PLA-based  
 142 composites at 58°C are characterized by a lower mass variation with respect to neat PLA. This effect  
 143 could be related to increased crystallinity of PLA due to fillers addition [31]. Visual observation of  
 144 samples is visible in figure 3, and agrees with mass variation results.

145

**Table 2.** SEC results for PLA-based samples after composting tests at 35°C and 58°C.

	$\overline{M}_w$ (Da)						
	35°C				58°C		
	t0	t1	t2	t3	t1	t2	t3
PLA	41832	41782	45782	44912	35324	8606	5083
PLA60-WF40	41925	41725	39316	39202	30179	18692	5334

PLA60-P40	43283	43052	43576	42529	34934	19898	5771
PLA60-WF30-P10	42274	42069	39060	38409	32402	23374	5222

146 Mass-average molecular weight ( $\overline{M}_w$ ) in mesophilic conditions (35°C) did not display sensitive  
 147 variations, suggesting a slow PLA degradation. In fact, the first step of PLA degradation is  
 148 characterized by hydrolysis. This process allows chain scissions until  $\overline{M}_w$  reach suitable chain length  
 149 for microorganisms attack [32]. Mesophilic condition seems to be insufficient to reduce PLA  $\overline{M}_w$   
 150 because of limited water diffusion and action on ester groups [33]. PLA-based composites, both with  
 151 wood flour and recycled waste paper, still display small Mw variations. PLA-based samples tested  
 152 in thermophilic conditions (58°C), conversely, displayed  $\overline{M}_w$  sensitive reduction by time: in fact,  $\overline{M}_w$   
 153 decreased from about 40kDa to about 5kDa after three months. PLA degradation hydrolytic step, in  
 154 agreement with literature results [34], is temperature sensitive, displaying optimal kinetic condition  
 155 around 58°C. However, recycled waste paper seems to partially hinder PLA degradation with respect  
 156 to wood flour, keeping  $\overline{M}_w$  at slightly higher values. In any case, the addition of cellulosic fillers  
 157 seems to increase PLA crystallinity, affecting water diffusion. As a consequence, a lower degradation  
 158 phenomenon is displayed by composites with respect to neat PLA [35-36].

159 Thermogravimetric analysis has been performed on pure HDPE and on HDPE composites filled  
 160 with wood flour and recycled paper, at time 0 and after 30, 60 and 90 days of composting at  
 161 temperatures of 35°C and 58 °C. Observing thermograms, the presence of fillers reduces thermal  
 162 stability of samples by lowering the onset temperature degradation compared to neat HDPE. Low  
 163 degradation temperatures of paper and wood flour are due to the presence of hemicellulose, cellulose  
 164 and lignin that are sensitive to thermal degradation [32-34, 37].

165 HDPE, for all time (table 3), as reported in literature [32-34, 37], is thermally stable up to  
 166 temperatures of about 450 °C and then quickly starts to degrade, with a maximum weight variation  
 167 speed around 480 °C. Samples do not display significant variations in both onset temperature and  
 168 temperature of the maximum weight variation for HDPE. The degradation leads, in all cases, to a  
 169 total loss of mass because of thermal cracking ending around about 500 °C [32-34, 37]. HDPE60-WF40  
 170 and HDPE60-P40 display a multistep thermal degradation (**Error! Reference source not found.** and  
 171 5). Firstly, moisture evaporation from room temperature to about 100°C. Secondly, thermal  
 172 degradation of hemicellulose, the most thermal sensitive component in lignocellulosic fillers [38],  
 173 occurs around 295°C. Cellulose pyrolysis is displayed at higher temperature range (315-400 °C) [37-  
 174 40], and around 350 °C the maximum thermal degradation rate of cellulose and lignin is displayed.  
 175 For temperatures higher than 400°C, almost all cellulose is pyrolyzed, while lignin decomposes more  
 176 slowly, over 400 °C and with a higher amount of solid residue. Samples display, considering  
 177 composting progression up to time 3, a modest reduction in the initial degradation temperature with  
 178 a reduction in the residual mass. HDPE60-P40, rich in cellulose, displays a residual mass  
 179 approximately unchanged at around 5%, while HDPE60-WF40, due to the higher lignin content,  
 180 displays higher residual mass [39]. Moreover, HDPE60-WF40 displays reduction of residual mass of  
 181 samples after composting process from 11% to 7%.

182 **Table 3.** TGA results for HDPE and PLA based composites after three months buried at 35°C and  
 183 58°C.

184 a) Tonset results, b) Tpeak results, c)  $\Delta m$  results.

185 a

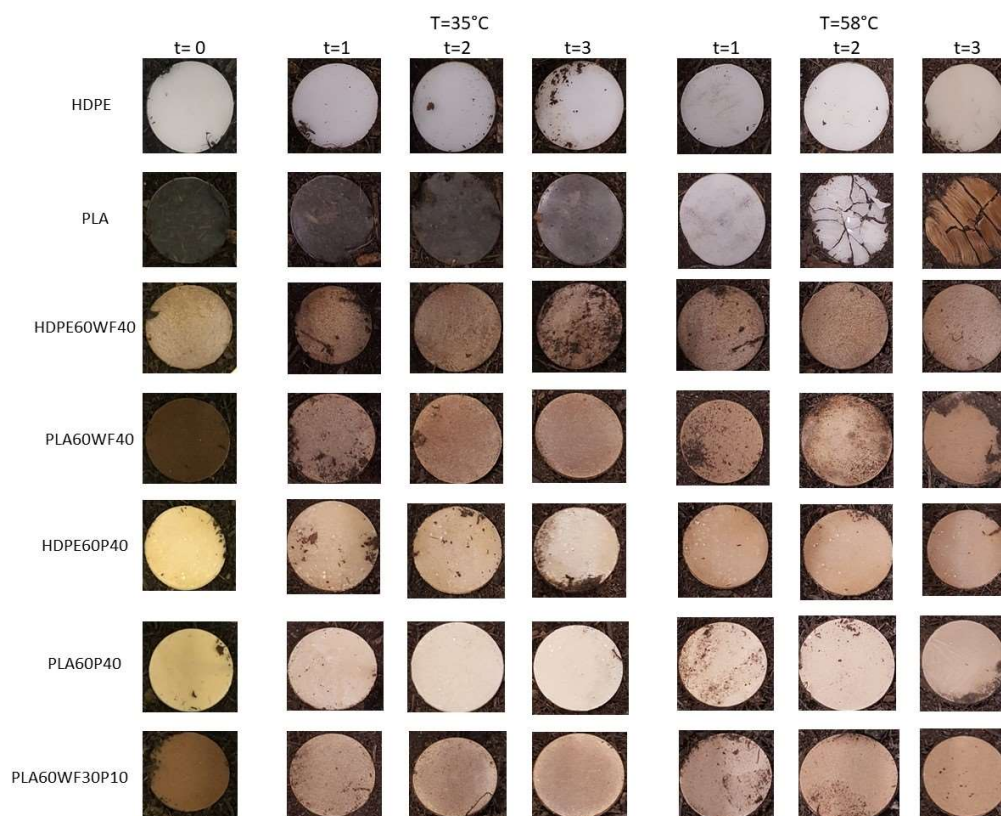
	35°C				58°C			
	t0	t1	Tonset (°C)		t1	Tonset (°C)		
			t2	t3		t2	t3	
HDPE	451	461	464	464	459	471	468	
HDPE60WF40	295	295	297	297	300	291	283	
HDPE60P40	313	14	304	308	305	294	298	

PLA	318	333	296	324	302	258	240
PLA60WF40	296	295	293	291	296	280	248
PLA60P40	323	318	309	315	297	297	242
PLA60WF30P10	301	307	299	297	298	297	254

b

	35°C				58°C			
	T <sub>peak</sub> (°C)							
	t0	t1	t2	t3	t1	t2	t3	
HDPE		477	481	481	481	479	484	484
HDPE60WF40	356/483	350/483	340/483	336/480	341/482	351/485	333/484	
HDPE60P40	344/484	346/483	336/483	346/484	333/484	326/477	320/298	
PLA		343	356	320	351	336	298	271
PLA60WF40		321	314	313	313	316	306	269
PLA60P40		344	337	330	333	316	324	264
PLA60WF30P10		327	327	321	316	321	307	275

	35°C				58°C			
	Δm (%)							
	t0	t1	t2	t3	t1	t2	t3	
HDPE		100	100	100	100	100	100	100
HDPE60WF40		91	89	90	93	91	91	91
HDPE60P40		95	94	95	95	93	94	93
PLA		100	100	100	100	100	100	100
PLA60WF40		89	88	88	91	90	91	96
PLA60P40		94	94	94	95	89	93	93
PLA60WF30P10		90	89	92	93	91	91	91



187  
188 *Figure 3.* Visual observation of samples at time 0, and after 1,2 and 3 months buried at 35°C and  
189 58°C.

190 PLA-based samples have also been analyzed by SEC in tetrahydrofuran, in order to evaluate  
191 average molecular weight variation during composting at 35°C and 58°C (Table 2).

192 **Table 2.** SEC results for PLA-based samples after composting tests at 35°C and 58°C.

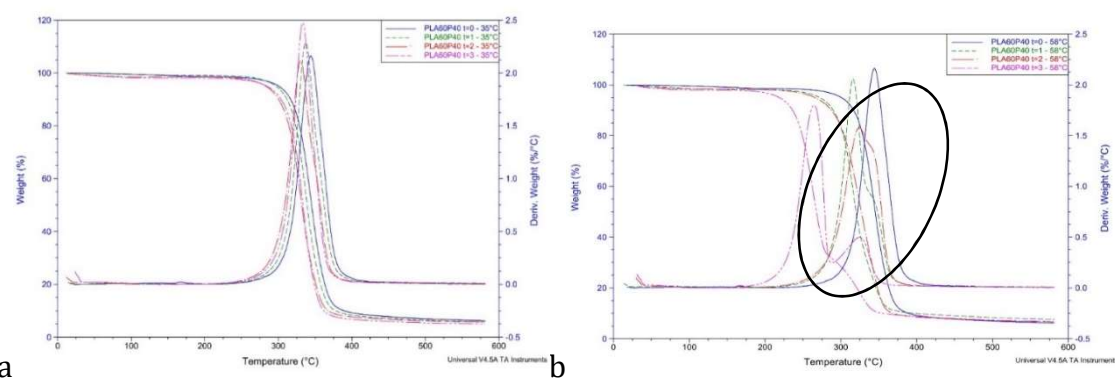
	$\overline{M}_w$ (Da)						
	35°C				58°C		
	t0	t1	t2	t3	t1	t2	t3
PLA	41832	41782	45782	44912	35324	8606	5083
PLA60-WF40	41925	41725	39316	39202	30179	18692	5334
PLA60-P40	43283	43052	43576	42529	34934	19898	5771
PLA60-WF30-P10	42274	42069	39060	38409	32402	23374	5222

193  
194 TGA curves of PLA display, over time, a significant difference in thermal stability between  
195 samples at 35 ° C compared to 58 ° C. Mesophilic conditions display a reduction of thermal stability  
196 only at time 3. Graphs display a single peak of maximum decomposition rate which starts at about  
197 320 ° C and at 350 ° C. PLA is completely degraded with no residual mass. Samples after burying at  
198 58 ° C, on the other hand, display a thermal stability reduction over time, possibly related to the  
199 presence of shorter macromolecules compared to time 0, because of degradation process [41]. The  
200 onset temperature at time 3 is about 240 ° C and, at 300 ° C, PLA is completely degraded with no  
201 residual mass.

202 The addition of wood flour, for samples buried at 35°C, reduces thermal stability of the  
203 composite compared to neat PLA. Samples buried at 58°C, on the other hand, display a progressive

204 reduction of stability over time, but higher than neat PLA. This trend is due to the hemicellulose and  
 205 PLA degradation during composting process. Thermograms display that thermal decomposition of  
 206 PLA60-WF40 composite occurs between 150 and 450°C. In mesophilic and even more evident in  
 207 thermophilic conditions, the presence of "shoulders" due to the overlapping of cellulose and lignin  
 208 bands is highlighted. PLA, under composting conditions, displays a reduction in onset temperature  
 209 degradation and sample is progressively more enriched in cellulose. As a consequence, after  
 210 composting process, two separate peaks are visible, the first refers to PLA and the second to cellulose  
 211 [42]. A residual mass is displayed at the end of thermal degradation, decreasing over time.

212 PLA60-P40 displays a reduction in thermal stability with respect to neat PLA. Thermograms  
 213 display a single peak for samples buried at 35°C, with a slight decrease in thermal stability over time.  
 214 Samples at 58°C display higher reduction of thermal stability and the appearance of shoulder, already  
 215 displayed for PLA60-WF40, becomes more visible over time (**Error! Reference source not found.**).  
 216 All samples display a reduction of onset temperature with respect to PLA60-WF40, possibly  
 217 associated with the lower presence of hemicellulose in paper. A residual mass is displayed at the end  
 218 of thermal degradation, in lower amount than PLA60-WF40, which remains stable over time due to  
 219 the lower presence of lignin and hemicellulose [43].



220

a

b

221 **Figure 4.** Mass and derivative variations in weight as a function of temperature during the  
 222 degradation of PLA60-P40 at month 0, 1, 2, 3 at 35 °C (a) and 58°C (b).

223 DSC analyses allow understanding the influence of natural fillers on both HDPE and PLA  
 224 thermal properties, but also the influence of composting process on materials. Neat HDPE display,  
 225 as expected, no sensitive variation of melting temperature after composting at both 35°C and 58°C.  
 226 HDPE-based composites with WF and P display higher melting and crystallization enthalpies values  
 227 compared to neat HDPE. Similar observations are in agreement with results of Lee et al., who have  
 228 studied the influence of different types of softwood in HDPE matrix composites [44]. This effect is  
 229 more evident for P than for WF, probably because of morphological differences between P (fibrous)  
 230 and WF (particulate). No sensitive variations are displayed with DSC analyses for HDPE-based  
 231 samples, probably because degradation mainly occurs on natural fillers, keeping unchanged HDPE.  
 232 No sensitive variations have been displayed for PLA after composting at 35°C and the curves are  
 233 almost superimposable, in agreement with no mass and Mw variation. Samples after composting at  
 234 58°C (**Error! Reference source not found.**), instead, as the composting process proceeds, show a  
 235 decrease in glass transition temperature (T<sub>g</sub>), from 61°C to about 40°C after three months. Moreover,  
 236 typical cold crystallization temperature (T<sub>cc</sub>) displays a decrease at 58°C during the degradation  
 237 process. This reduction may be associated with the formation of oligomers of lactic acid resulting  
 238 from the cleavage of chains due to hydrolysis during composting, as confirmed also by Mw  
 239 reduction. Chains with lower molecular mass crystallize more easily and have lower cold  
 240 crystallization temperatures [45]. No crystallization during cooling has been detected during DSC  
 241 analyses for neat PLA.

242

**Table 4.** DSC results for neat PLA during composting process at 58°C.

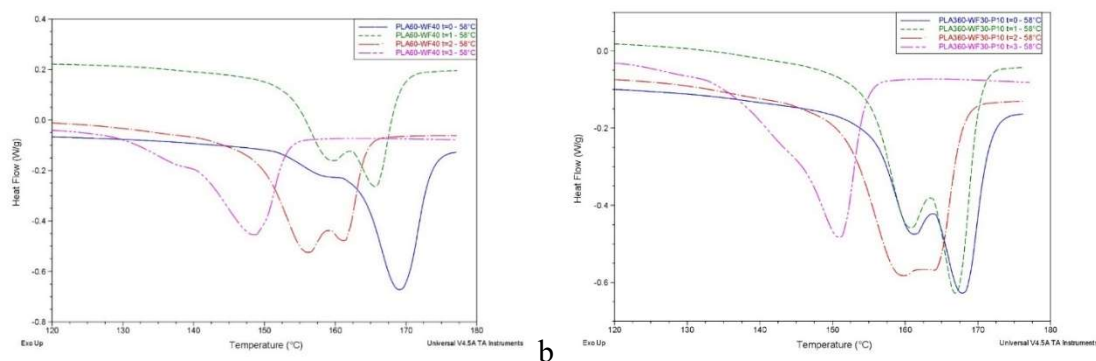
	<b>T<sub>m</sub></b> (°C)	<b>ΔH<sub>m</sub></b> <b>PLA</b> (J/g <sub>PLA</sub> )	<b>T<sub>cc</sub></b> (°C)	<b>T<sub>g</sub></b> (°C)
PLA t0	169	48	100	61
PLA t1	166	53	94	55
PLA t2	148	47	84	45
PLA t3	144	45	90	41

243 The presence of wood flour and recycled waste paper in PLA60-WF40, PLA60-P40 and PLA60-  
 244 WF30-P10 seems to obstacle cold crystallization, not detected for these samples, because of nucleating  
 245 effect of natural fillers, facilitating crystallinity from molten state. As a consequence, a formation of  
 246 two melting peaks was evident (as visible from **Error! Reference source not found.**), indicating the  
 247 presence of two crystalline fractions. Moreover, thermograms of samples buried at 35 °C are almost  
 248 superimposable for all composites, while at 58°C there is a displacement of melting peaks towards  
 249 lower temperatures.  $\overline{M}_w$  reduction, due to degradation progression, is responsible for T<sub>g</sub>, T<sub>cc</sub> and  
 250 T<sub>m</sub> reduction. In fact, the lower chain length, the easier the chain mobility [46]. In fact, under  
 251 mesophilic conditions, melting temperature T<sub>m</sub> does not show significant variations compared to  
 252 neat PLA. Samples buried under thermophilic condition display a significant reduction of T<sub>m</sub> over  
 253 time (**Error! Reference source not found.**). This reduction is analogous to the one displayed by neat  
 254 PLA, and is probably associated with a decrease in M<sub>w</sub>, although T<sub>m</sub> of PLA-based composites are  
 255 still higher than T<sub>m</sub> of PLA.

256

**Table 5.** DSC results for PLA-based composites during composting process at 58°C.

	<b>T<sub>m</sub></b> (°C)	<b>ΔH<sub>m</sub></b> <b>PLA</b> (J/g <sub>PLA</sub> )
PLA60-WF40 t0	169	54
PLA60-WF40 t1	166	53
PLA60-WF40 t2	156	69
PLA60-WF40 t3	148	45
PLA60-P40 t0	171	53
PLA60-P40 t1	168	59
PLA60-P40 t2	162	62
PLA60-P40 t3	153	56
PLA60-WF30-P10 t0	168	55
PLA60-WF30-P10 t1	167	62
PLA60-WF30-P10 t2	160	69
PLA60-WF30-P10 t3	151	47



257

a

b

258

**Figure 5.** Melting peak of PLA60-WF40 (a) and PLA60-WF30-P10 (b) composites during composting process at 58°C.

259

260

261

262

263

264

265

266

267

268

269

270

271

272

273

274

275

276

277

278

279

280

281

282

283

284

285

286

287

288

289

290

291

292

293

294

295

296

FTIR analyses validate the others obtained results. HDPE did not display any modification of its spectra after three months buried in soil at both 35°C and 58°C. Spectra of HDPE60-P40 combine the absorption bands of HDPE matrix and characteristic absorption peaks of cellulose. Paper consists mainly of cellulose fibres but also contains hemicellulose and lignin [47]. Cellulose is characterized by a) peak at 1425 cm<sup>-1</sup>, known as the crystalline band, caused by the vibrations of the aromatic skeleton combined with the bending of the C-H (a lowering of its intensity reflects the decrease in the degree of crystallinity of samples), b) peak at 1032 cm<sup>-1</sup>, associated both with the symmetrical CO stretching of the cellulose and with the CO deformation of the primary alcohols in the lignin, c) peaks between 3400-3300 cm<sup>-1</sup> and 1593 cm<sup>-1</sup> attributed to the stretching and bending, respectively, of OH groups of cellulose [47-49]. This modification, together with the shift of peak at 1316 cm<sup>-1</sup> towards higher values, denotes the development of new inter- and intramolecular hydrogen bonds. The predominant degradation phenomenon that characterizes the filler is oxidative [50], especially for hemicellulose and lignin. The oxidative process is detected by increasing intensity of the small peaks generated by the functional carbonyl group in the absorption range between 1800-1600 cm<sup>-1</sup>. In particular, small signals revealed in the area 1740-1709 cm<sup>-1</sup> are an expression of the carbonyl groups related to C = O stretching of hemicellulose groups or to the ester bond of the carboxylic group in the ferulic and coumarinic acids of the lignin and hemicellulose. This also makes this zone a good "marker" of oxidative processes, the intensity of the band around 1735 cm<sup>-1</sup> is usually proportional to the oxidation of hemicellulose (C = O in xylan). The areas of interest for PLA at about 1750 and 1180 cm<sup>-1</sup> are clearly visible, which belong to the stretching C-O and to the stretching C-O-C of PLA. 1080 cm<sup>-1</sup> is associated to the C-C stretching. The biodegradation of polylactic acid should determine an increase of carboxylic and alcoholic groups. Over time, at 35 ° C, there are no evident peaks variation, while at 58 ° C, as the biodegradation process proceeds, PLA displays a variation related to the peak at 1750 cm<sup>-1</sup> due to the stretching of the C = O group. PLA biodegradation is highly sensitive to moisture, obtaining a degradation process characterized by water absorption, ester cleavage forming oligomers, solubilization of oligomer fractions and diffusion of bacteria into soluble oligomers [51]. Biodegradation of PLA should lead to an increase in carboxylic and alcoholic groups. In fact, a shift of the peak at 1750 cm<sup>-1</sup>, assigned to the stretching of the carbonyl, confirms a successful degradation. WF probably accelerated the degradation of composite during composting at 35°C, over time enriched in WF. The explanation would be attributed to a greater degradation by hydrolysis of PLA due to the presence of moisture in the wood [52]. Degradation of PLA, also for PLA60-P40, can be associated with the increase of the terminal hydroxyl peak and the variation, although not always linear (probably due to the lack of homogeneity of the sample), of the peak in the area between 1730 and 1750 cm<sup>-1</sup>, characteristic of carbonyl groups related to C = O stretching. An increase in terminal hydroxyl peak is in agreement with a reduction in molecular mass. In conclusion, as expected, pure HDPE was non-biodegradable, while HDPE60-WF40 and HDPE60-P40 display only degradation of cellulose, lignin and hemicellulose. Neat PLA sample at 35 ° C was not very sensitive

297 to degradation processes, but biodegradation was accelerated by the presence of paper and/or wood  
 298 flour. At 58°C, pure PLA is easily biodegradable, and signs of biodegradation increase over time.  
 299 PLA-based composites are characterized by PLA degradation and enrichment in cellulose, less  
 300 sensitive to biodegradation.

#### 301 4. Conclusions

302 HDPE-based and PLA-based composites have been tested to analyze the effect of natural fillers  
 303 (wood flour, recycled waste paper and a mix of both fillers) on polymer degradation. Moreover,  
 304 samples made of HDPE-PLA blend and a mix of two fillers have also been tested. Future studies have  
 305 to be done in order to complete the study on the effect of these fillers on HDPE and PLA composting  
 306 features. In fact, PLA is sensitive to temperature and humidity conditions, displaying higher  
 307 reduction of Mw when composting is performed at 58°C. Moreover, natural fillers seem to influence  
 308 mass variation, already at 35°C. In fact, degradation of fillers at 35°C allows a mass reduction during  
 309 composting of composites, while neat PLA do not display any variation. These results are in  
 310 agreement with other analyses performed (TGA, DSC), validating natural filler degradation under  
 311 composting conditions.

312 **Conflicts of Interest:** The authors declare no conflict of interest.

#### 313 References

- 314 1. Speight, J. G., Monomers, Polymers, and Plastics. *Handbook of Industrial Hydrocarbon Processes*, **2011**, 499–  
 315 537.
- 316 2. Gajjar, C.R.; King, M.W., Degradation Process in Resorbable Fiber-Forming Polymers for Biotextile  
 317 Applications, *Materials*, **2004**.
- 318 3. Vasile, C., Role of the polymer degradation processes in environmental pollution and waste treatment,  
 319 *Polimery*, **2002**, 8, 517.
- 320 4. Kulkarni, A.; Dasari, H., Current Status of Methods Used in Degradation of Polymers: A review, *MATEC*  
 321 *Web of Conferences*, **2018**, 144.
- 322 5. Engineer, C.; Parikh, J.; Raval, A, Review on Hydrolytic Degradation Behavior of Biodegradable Polymers  
 323 from Controlled Drug Delivery System, *Trends Biomater. Artif. Organs*, **2001**, 25, 79-85.
- 324 6. Tiwari, A.K.; Gautam, M.; Maurya H.K, Recent Development of Biodegradation Techniques of Polymer,  
 325 *Int. J. Res. Granthaalayah*, **2018**, 6.
- 326 7. Gu J.D., Microbiological deterioration and degradation of synthetic polymeric materials: recent research  
 327 advances, **2003**, *Int. Biodet. Biodeg*, 52, 69-91.
- 328 8. McKew, B.A.; Dumbrell, A.J.; Taylor, J.D.; McGenity, T.J.; Underwood, G.J.U, Differences between aerobic  
 329 and anaerobic degradation of microphytobenthic biofilm-derived organic matter within intertidal  
 330 sediments, *FEMS Microbiology Ecology*, **2013**, 84, 495-509.
- 331 9. Bajpai, M, Basics of Anaerobic Digestion Process, *Anaerobic Technology in Pulp and Paper Industry*, **2017**, 7-  
 332 12.
- 333 10. Doble, M.; Kumar A., Aerobic and Anaerobic Bioreactors, in *Biotreatment of Industrial Effluents*, **2005**, 19-38
- 334 11. Boonmee, C.; Kositanont, C.; Leejarkpai, T., Degradation of Poly (Lactic Acid) under Simulated Landfill  
 335 Conditions, *Env. Nat. Res. J.*, **2016**, 14, 1-9.
- 336 12. Massardier, V.; Pestre, C.; Cruard-Pradet, T.; Bayard, R., Aerobic and anaerobic biodegradability of  
 337 polymer films and physico-chemical characterization, *Pol. Deg. St.*, **2006**, 91, 620-627.
- 338 13. Arkatkar, A.S.; Arutchelvi, J.; Muniyasamy, S.; Bhaduri, S.; Uppara, P.V.; Doble, M., Approaches to Enhance  
 339 the Biodegradation of Polyolefins, *The Open Environmental Engineering Journal*, **2009**, 2, 68.
- 340 14. Sinclair, R.G., Blends of polyactic acid, **1993**, Patent US5216050A.
- 341 15. As'habi, L.; Jafari, S.H.; Khonakdar, H.A.; Boldt, R.; Wagenknecht, U.; Heinrich, G., Tuning the  
 342 processability, morphology and biodegradability of clay incorporated PLA/LLDPE blends via selective  
 343 localization of nanoclay induced by melt mixing sequence, *Polym. Lett.*, **2013**, 7, 21-39.
- 344 16. Quitadamo, A.; Massardier, V.; Valente, M., Interactions between PLA, PE and wood flour:effects of  
 345 compatibilizing agents and ionic liquid , *Holz.*, **2017**, 72, 691-700.
- 346 17. Quitadamo, A.; Massardier, V.; Valente, M. Optimization Of Thermoplastic Blend Matrix HDPE/PLA With  
 347 Different Nature And Level Of Coupling Agent, *Materials* **2018**, 11, 2527; doi:10.3390/ma11122527.

- 348 18. Quitadamo, A.; Massardier, V.; Valente, M. Oil-based/Bio-Derived Thermoplastic Polymer Blends and  
349 Composites, **2018**, In *Introduction to Renewable Biomaterials: First Principles and Concepts*, Lucia, L.; Ayoub,  
350 A.; Wiley Hoboken, New Jersey, USA, 239-268.
- 351 19. Boubekour, B.; Belhaneche Bensemra, N.; Massardier, V., Valorization of waste jute fibers in developing  
352 low-density polyethylene/ polylactic acid bio-based composites, *J. Reinf. Plast. Comp.*, **2015**, *34*, 649-661.
- 353 20. Valente, M.; Tirillò, J.; Quitadamo, A.; Santulli S., Paper fiber filled polymer. Mechanical evaluation and  
354 interfaces modification, *Compos Part B-Eng.*, **2017**, *110*, 520-529.
- 355 21. Mohanty, A.K.; Mistra, M.; Hinrichsen, G., Biofibres, biodegradable polymers and biocomposites: An  
356 overview, *Macromol. Mater. Eng.*, **2000**, *276*, 1-24.
- 357 22. Gurunathan, T.; Mohanty, S.; Nayak, S.K., A review of the recent developments in biocomposites based on  
358 natural fibres and their application perspectives, *Compos. Part A-Appl. Sci.*, **2015**, *77*, 1-25.
- 359 23. Rowell, R.M.; Stout, H.P., Jute and Kenaf. In: *Handbook of fibre chemistry*, **2007**, M. Lewin, 405-452, ed Vol. 3,  
360 Boca Raton, FL: CRC Press.
- 361 24. Saha, P.; Manna, S.; Roy, D.; Chowdhury, S.; Kim, K.G.; Banik, S.; Adhiikari, B.; Kim, J.K., Biodegradation  
362 of Chemically Modified Jute Fibres, *J. Nat. Fib.*, **2015**, *12*, 542-551.
- 363 25. Itavaara, M.; Karjomaa, S.; Selin, J.F., Biodegradation of polylactide in aerobic and anaerobic thermophilic  
364 conditions, *Chemosphere*, **2002**, *46*, 879-885.
- 365 26. Orhan, Y.; Hrenovic, J.; Buyukgungor, J.H., Biodegradation of plastic compost bags under controlled soil  
366 conditions., *Acta Chim. Slov.*, **2004**, *51*, 579-588.
- 367 27. Nourbakhsh, A.; Ashori, A.; Tabrizi, A.K., Characterization and biodegradability of polypropylene  
368 composites using agricultural residues and waste fish, *Compos. Part B-Eng.*, **2014**, *56*, 279-283.
- 369 28. Praprudivongs, A.; Sombatsompop, N., Biodegradation and Anti-bacterial Properties of PLA and  
370 Wood/PLA Composites Incorporated with Zeomic Anti-bacterial Agent., *Adv. Mat. Res.*, **2013**, *747*, 111-114.
- 371 29. Queirós, Y. G. C.; Machado, K. J. A.; Costa, J. M.; Lucas, E. F., Brazilian synthesis, characterization, and  
372 in vitro degradation of poly(lactic acid) under petroleum production conditions, *J. Petrol. Gas*, **2013**, *7*, 57-69.
- 373 30. Ke, T.; Sun, X., Melting behaviour and crystallization kinetics of starch and poly(lactic acid) composites, *J.*  
374 *App. Polym. Sci.*, **2003**, *89*, 1203-1210.
- 375 31. A.P. Mathew, K. Oksman, M.Sain, The effect of morphology and chemical characteristics of cellulose  
376 reinforcements on the crystallinity of polylactic acid, *J. App. Polym. Sci.*, **2006**, *101*, 300-310.
- 377 32. Ndazi, B.S.; Karlsson, S.; Characterization of hydrolytic degradation of polylactic acid/rice hulls composites  
378 in water at different temperatures, *Express Polym. Sci.*, **2011**, *5*, pp. 119-131.
- 379 33. Kolstad, J.K.; Vink, E.T.H.; De Wilde, B.; Debeer, L. Assessment of anaerobic degradation of Ingeo  
380 polylactides under accelerated landfill conditions, *Poly. Degrad. St.*, **2012**, *97*, 1131-1141.
- 381 34. Itavaara, M.; Karjomaa, S.; Selin, J.F. Biodegradation of polylactide in aerobic and anaerobic thermophilic  
382 conditions, *Chemosphere*, **2006**, *46*, 879-885.
- 383 35. Fortunati, E.; Luzi, F.; Puglia, D.; Dominici, F.; Santulli, C.; Kenny, J.M.; Torre, L. Investigation of thermo-  
384 mechanical, chemical and degradative properties of PLA-limonene films reinforced with cellulose  
385 nanocrystals extracted from Phormium tenax leaves, *Europ. Polym. J.*, **2014**, *56*, 77-91.
- 386 36. Luzi, F.; Fortunati, E.; Puglia, D.; Petrucci, R.; Kenny, J.M.; Torre, L. Study of disintegrability in compost  
387 and enzymatic degradation of PLA and PLA nanocomposites reinforced with cellulose nanocrystals  
388 extracted from Posidonia Oceanica, *Polym Degrad. St.*, **2015**, *121*, 105-115.
- 389 37. Liu, R.; Cao, J.; Ouyang, L. Degradation of wood flour/poly (lactic acid) composites reinforced by coupling  
390 agents and organo-montmorillonite in a compost test., *Wood Fiber Sci*, **2018**, *45*, 105-118.
- 391 38. Banat, R.; Fares, M.M.; Thermo-Gravimetric Stability of High Density Polyethylene Composite Filled with  
392 Olive Shell Flour., *Am. J. Polym. Sci.*, **2015**, *5*, 65-74.
- 393 39. Paabo, M.; Levin, B.C. A Literature Review of the Chemical Nature and Toxicity of the Decomposition  
394 Products of Polyethylenes., *Fire Mater*, **1987**, *11*, 55-70.
- 395 40. Mengeloglu, F.; Karakus, K.; Thermal Degradation, Mechanical Properties and Morphology of Wheat  
396 Straw Flour Filled Recycled Thermoplastic Composites., *Sensors*, **2008**, *8*, 500-519.
- 397 41. Krehula, L.L.; Katancic, Z.; Sirocic, A.P.; Hrnjak-Murgic, Z. Weathering of high density polyethylene-wood  
398 plastic composites, *J. Wood. Chem. Technol.*, **2014**, *34*, 39-54.
- 399 42. Yang, H.; Yan, R.; Chen, H.; Ho Lee, D.; Zheng, C.; Characteristics of hemicellulose, cellulose and lignin  
400 pyrolysis, *Fuel*, **2007**, *86*, 1781-1788.
- 401 43. Watkins, D.; Nuruddin, M.D.; Hosur, M.; Extraction and characterization of lignin from different biomass  
402 resources, *J. Mater. Res. Tech.*, **2015**, *4*, 26-32.
- 403 44. Kim, H.S.; Yang, H.S.; Kim, H. J.; Park, H.J. Thermogravimetric Analysis of Husk Flour Filled Thermoplastic  
404 Polymer Composites, *J. Therm. Anal. Calorim.*, **2004**, *76*, 395-404.

- 405 45. Espert, A.; Camacho, W.; Karlson, S. Thermal and Thermo Mechanical Properties of Biocomposites Made  
406 from Modified Recycled Cellulose and Recycled Polypropylene, *J. Appl. Polym. Sci.*, **2003**, 89, 2353–2360.
- 407 46. De Bartolo, L, Curcio, E., Drioli, E., Membrane Systems: for bioartificial organs and regenerative medicine,  
408 *De Gruyter*, **2017**
- 409 47. Liao, Q.J.; Jiang, Y.C.; Turg, L.S.; Chen, C.C. Biodegradability of PLA in compost environment., *SPE*  
410 *ANTEC Anaheim*, **2017**.
- 411 48. Lee, S.H.; Wang, S. Biodegradable polymers/bamboo fiber biocomposite with biobased coupling agent.,  
412 *Compos. Part A-Appl. S.*, **2006**, 37, 80-91.
- 413 49. Zimmermann, M.V.G.; Brambilla, V.C.; Brandalise, B.M.; Zattera, A.J. Observations of the Effects of  
414 Different Chemical Blowing Agents on the Degradation of Poly(Lactic Acid) Foams in Simulated Soil., *Mat.*  
415 *Res.*, **2013**, 16, 1266-1273.
- 416 50. V.K.; O'Donovan, A.; Tuohy, M.G.; Sharma, G.D. Trichoderma in bioenergy research: An overview, in  
417 *Biotechnology and Biology of Trichoderma*, Druzhinina I.; Herrera-Estrella, A.; Gupta, V.K.; Tuohy M.G., 2014
- 418 51. Liu, R.; Cao, J.; Ouyang, L. Degradation of wood flour/poly (lactic acid) composites reinforced by coupling  
419 agents and organo-montmorillonite in a compost test., *Wood Fiber. Sci.*, **2018**, 45, 105-118.
- 420 52. R.B. Santos R. B.; Capanema E.A., Balakshin M.Y., Chang H., Jameel, H. Lignin Structural Variation in  
421 Hardwood Species; *J. Agr. Food Chem*, 2012, 60, 4923-4930.